

# RSC Advances



This is an *Accepted Manuscript*, which has been through the Royal Society of Chemistry peer review process and has been accepted for publication.

*Accepted Manuscripts* are published online shortly after acceptance, before technical editing, formatting and proof reading. Using this free service, authors can make their results available to the community, in citable form, before we publish the edited article. This *Accepted Manuscript* will be replaced by the edited, formatted and paginated article as soon as this is available.

You can find more information about *Accepted Manuscripts* in the [Information for Authors](#).

Please note that technical editing may introduce minor changes to the text and/or graphics, which may alter content. The journal's standard [Terms & Conditions](#) and the [Ethical guidelines](#) still apply. In no event shall the Royal Society of Chemistry be held responsible for any errors or omissions in this *Accepted Manuscript* or any consequences arising from the use of any information it contains.

Cite this: DOI: 10.1039/c0xx00000x

www.rsc.org/xxxxxx

ARTICLE TYPE

## Water soluble Calcium-Sodium based coordination polymer: Selective Release of Calcium at Specific Binding Sites on Protein

Ruchi Gaur<sup>a,‡</sup>, Ambadipudi Susmitha<sup>a,b,‡</sup>, K V R Chary<sup>b</sup> and Lallan Mishra<sup>a\*</sup>

Received (in XXX, XXX) Xth XXXXXXXXX 20XX, Accepted Xth XXXXXXXXX 20XX

DOI: 10.1039/b000000x

A calcium-sodium based water soluble coordination complex  $[\{Ca_4Na(EGTA)_2(H_2O)_{13}\}_n \cdot NO_3]$  (EGTA = ethylene bis(oxyethylenitrilo)tetraacetic acid) henceforth named Ca/Na-1, has been synthesized hydrothermally and characterized using spectroscopic and single crystal X-ray diffraction techniques. Single crystal X-ray diffraction of the assembly affirms two dimensional self assembled net like supra molecular structure. The complex serves as a biological mimic of calcium buffer and dispenses felicitous amounts of  $Ca^{2+}$  ions at the binding sites on protein, supported by SEM image and MALDI-TOF spectroscopy. The thermodynamics of binding has also been measured by isothermal titration calorimetry. Protein conformational changes have been characterized by NMR spectroscopy.

Over past few decades, the field of coordination polymers has picked up attention their structural richness and promising applications in supramolecular chemistry, catalysis, drug delivery, gas storage, separation and sensors.<sup>1</sup> Careful selection of metal ion connectors like Zn, Cu, Mn, Ca, Pd, Pt, Fe and Cd into poly-dentate bridging ligand containing N and O donors has facilitated the evolution of coordination polymers with versatile functionality.<sup>2</sup> The multicarboxylic acids are mostly used as linkers for the assembly owing to variety of coordination modes for the formation of diverse multidimensional architectures.<sup>3</sup> Despite the large diversity, utility of coordination polymers is limited in biomedical applications due to their insolubility, toxicity, degradability and lack of suitable techniques for their functional detection. In this context, recent studies have proposed suitable combination of nontoxic and biocompatible cations such as  $Na^+$ ,  $Zn^{2+}$ ,  $Fe^{2+}$  and  $Ca^{2+}$  couple directly with functionalized and therapeutically active linkers in the construction of coordination polymers.<sup>1,4</sup> For the drug development approach, tremendous efforts have led to the design of molecules to encapsulate calcium, and more importantly, to capture and release calcium. Within the cell milieu, free calcium is excluded from the cytoplasm since  $Ca^{2+}$  binds less tightly to water and precipitates various cellular phosphates. This exclusion is accomplished by specialized  $Ca^{2+}$  binding proteins (CaBPs) whose binding affinities for  $Ca^{2+}$  range from nM to mM.<sup>5</sup> Here, the active site carboxyl and carbonyl groups of the CaBPs serve as chelating centres and form co-ordination sphere with  $Ca^{2+}$ . Several BAPTA based photo induced  $Ca^{2+}$  chelators have also been proposed for selective triggering and mapping of  $Ca^{2+}$  inside the cells.<sup>5</sup> Though coordination polymers were exploited in almost every field of research, coordination polymer-protein interactions and metal

ions release are still unexplored. In this context, we present a rational design for the incorporation of Ca and Na into EGTA framework for selective release and targeted delivery of Ca at designated sites on protein.

The ligand EGTA was selected owing to its biodegradable and flexible framework with a variety of coordination modes which are anticipated to provide multidimensional architecture.<sup>6</sup> It is also established that EGTA strongly binds  $Ca^{2+}$  in 1:1 stoichiometry with dissociation constant ( $K_d$ ) in the order of nM and can mimic the intracellular environment.<sup>7</sup> In this backdrop, we designed a strategy to alter the stoichiometry of calcium per molecule of EGTA, to increase the  $K_d$  of Ca-EGTA complexation. This can be achieved through the exploitation of flexible bidentate arms of EGTA to anchor additional metal ions. An optimal reduction in the affinity is expected to confer  $Ca^{2+}$  releasing ability to EGTA in presence of ligands with higher affinity for  $Ca^{2+}$  ions.

Synthesis of the proposed complex  $[\{Ca_4Na(EGTA)_2(H_2O)_{13}\}_n \cdot NO_3]$  was carried out hydrothermally by reacting  $Ca(NO_3)_2 \cdot 4H_2O$  with EGTA in presence of NaOH (detailed procedure is described in Supplementary information S1). Single crystal X-ray diffraction suggests that the structure of Ca/Na-1 crystallizes in monoclinic crystal system with space group  $P21/c$  as shown in Figure 1A. Data collection and structure refinement parameters, bond length and bond angle data are shown in Supplementary Tables 1 and 2 (S2 & S3). An asymmetric unit of each EGTA anion acts as octadentate ligand connecting four metal centers (three Ca(II) ions and one Na ion) and form a cage like structure with co-crystallized nitrate molecule. Two Ca(II) ions (Ca1 and Ca3) are equatorially connected in octa-coordinated fashion and bind six oxygen atoms from the carboxylate groups and two nitrogen atoms belonging to same EGTA ligand with the typical Ca-O bond length values ranging from 2.363(5) to 2.592(5) Å and fall in the reported range.<sup>8</sup> Two Ca(II) centers coordinated with carboxylate dianions of EGTA are bridged by other Ca(II) and Na (I) ions and are separated by a distance of 8.179 Å. In this way, the two  $EGTA^{4-}$  ligands link the metal ions acting as the building blocks forming cage with a 13-membered metallocycle. Overall, thirteen disordered coordinated water molecules are present in the Ca/Na-1. Further, Ca/Na-1 is interconnected and provides extended 2D net like supramolecular framework as depicted in Figure 1B. Solvent accessible volume calculated by PLATON analysis<sup>9</sup> is  $6013 \text{ \AA}^3$ , which is 14.5 % of the unit cell volume.

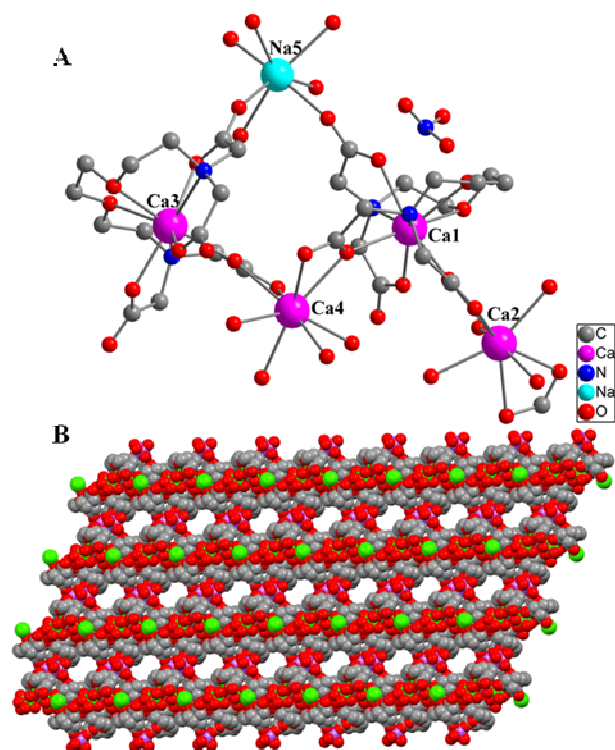


Figure 1. (A) Cage like asymmetric unit of Ca/Na-1 (Hydrogen omitted for clarity) (B) 2D mesh like structure of Ca/Na-1.

A characteristic peak of  $\nu_{as}(\text{COO}^-)$  vibration of free ligand observed at  $1744\text{ cm}^{-1}$  shifted to  $1635\text{ cm}^{-1}$  in the infrared spectrum of Ca/Na-1. The  $\nu_s(\text{COO}^-)$  is at  $1384\text{ cm}^{-1}$  and blue-shifts  $17\text{ cm}^{-1}$  compared to that of EGTA ( $1401\text{ cm}^{-1}$ ), supporting the co-ordination of deprotonated ligand to the metal ions in the complex.<sup>10</sup> MALDI-TOF mass spectrometry of Ca/Na-1 recorded in Tris-HCl buffer (pH 7.4) and 100 mM NaCl, showed a peak at 1232.19 corresponding to its parent molecular ion (Supplementary Figure 1, S4). The higher polymers could not be detected. The absence of larger fragments may be due to the rupture of metal/ligand bond under the conditions applied.<sup>11</sup> However, the isolation of the same complex from its solution in water supported the intactness of Ca/Na-1 even after dissolution in water. The UV-visible absorption and emission spectra are shown in Supplementary Figure 2 (S5). Electronic absorption spectrum shows peaks at  $\lambda_{\text{max}}$  302, 354, and 388 nm, assigned to  $\pi\text{-}\pi^*$  transitions and  $n\text{-}\pi^*$  transition of carboxylate groups respectively. An intense emission peak is displayed at  $\lambda_{\text{max}}$  452 nm on excitation at  $\lambda_{\text{max}}$  388 nm. The emission arises from the ligand centre.<sup>12</sup> To check the stoichiometric effect on the structure, UV-vis titration of 10 mM EGTA solution with different equivalents of  $\text{Ca}(\text{NO}_3)_2 \cdot 4\text{H}_2\text{O}$  in presence of 40 mM NaOH was carried out (Supplementary Figure 3, S6). No significant changes in the spectral features were observed, supporting that observed stoichiometry is almost stable. The 1D- $^1\text{H}$ ,  $^{13}\text{C}$  and  $^{23}\text{Na}$  NMR spectra of Ca/Na-1 are recorded in Tris-HCl buffer (pH 7.4) with 10%  $\text{D}_2\text{O}$  (Supplementary Figure 4, S7). Combined chemical shifts for  $^1\text{H}$  and  $^{13}\text{C}$  spectra are listed in Supplementary Table 3 (S8). The peaks at 180.41, 69.14, 68.18, 61.82 and 57.56 ppm correspond to carboxy groups ( $-\text{CO}_2$ ),  $\text{CH}_2$  groups of ( $-\text{NCH}_2\text{CO}_2$ ),  $\text{CH}_2$  groups of ( $-\text{O}-\text{CH}_2-\text{CH}_2$ ) and  $\text{CH}_2$  groups of acetates ( $-\text{NCH}_2\text{CH}_2-$ ), respectively. A shift of  $\delta$  0.967 ppm corresponding to single peak of  $^{23}\text{Na}$  compared to standard NaOH indicated the presence of Na in the Ca/Na-1. Incorporation of Ca

into coordination polymer was indirectly verified, since  $^{40}\text{Ca}$  was used for synthesis (as  $^{40}\text{Ca}(\text{NO}_3)_2 \cdot 4\text{H}_2\text{O}$ , >99 % pure).

As described earlier, it could be hypothesized that molecular asymmetry might result in lowering of binding affinity of either one or more Ca in Ca/Na-1. To test the hypothesis, Ca/Na-1 was titrated against a  $\beta/\gamma$ -crystallin protein, M-crystallin. This protein has two asymmetric motifs that bind  $\text{Ca}^{2+}$  ions with moderate and low binding affinities respectively. Also, it undergoes subtle conformational changes upon binding to  $\text{Ca}^{2+}$ .<sup>13</sup> Overlay of sensitivity enhanced 2D- $^{15}\text{N}$ - $^1\text{H}$  heteronuclear single quantum correlation (HSQC) spectra of the protein in presence and absence of Ca/Na-1 showed perturbation in amide proton chemical shifts (Figure 2).  $\text{Ca}^{2+}$  binds to M-crystallin with pentagonal bipyramidal geometry at site 1 and octahedral geometry at site 2 along with three coordinating water molecules.<sup>14</sup> For the reference, spectra were recorded using standard  $\text{CaCl}_2$  as titrant (Supplementary Figure 5, S9). The results corroborate the release of  $\text{Ca}^{2+}$  by Ca/Na-1 during titration with concomitant conformational changes in the protein. However, no significant change occurs in  $^{23}\text{Na}$  NMR spectrum of the Ca/Na-1 (Figure 3A) in the presence of protein supporting that  $\text{Na}^+$  ion remains intact during the release of  $\text{Ca}^{2+}$  ions.

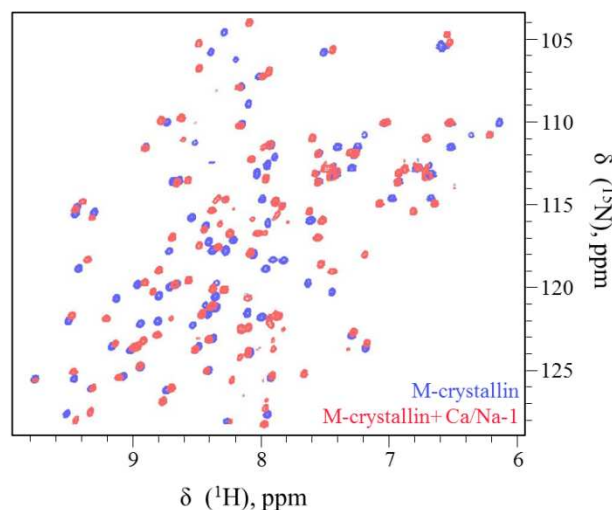


Figure 2. NMR titration of Ca/Na-1 with M-crystallin. Overlay of sensitivity enhanced  $^{15}\text{N}$ - $^1\text{H}$  HSQC spectra of free protein (blue) and Ca/Na-1 bound protein (red). Spectra were recorded at  $25\text{ }^\circ\text{C}$  in 25 mM Tris-HCl buffer (pH 7.4) and 100 mM NaCl.

The extent of interaction of Ca/Na-1 with M-crystallin and the binding energetics were estimated from isothermal titration calorimetry (ITC) profile. The overall dissociation constant ( $K_d$ ) is  $52\text{ }\mu\text{M}$  and best fitted to a two-site sequential binding model (Figure 3B). The individual dissociation constants were  $19\text{ }\mu\text{M}$  and  $147\text{ }\mu\text{M}$  and binding of  $\text{Ca}^{2+}$  at both the sites was enthalpically and entropically favored (Supplementary Table 4, S10). For comparison, ITC experiments repeated under identical conditions using 1 mM  $\text{CaCl}_2$  yielded a  $K_d$  of  $82.3\text{ }\mu\text{M}$ , consistent with the reported value.<sup>13</sup> Most plausible rationale for the release of free  $\text{Ca}^{2+}$  from Ca/Na-1 can be deduced from the fact that the activation enthalpy and entropy ( $\Delta H$  and  $\Delta S$ ) for  $\text{Ca}^{2+}$  exchange between EGTA and M-crystallin are distinct and are in favor of the protein. Also, the decreased binding affinity of Ca/Na-1 to  $\text{Ca}^{2+}$  can be ascribed to the asymmetry of metal centers in the complex. Noteworthy to mention in this context, is the difference in thermodynamic parameters, which can be attributed to anion effect in the titrant ( $\text{OH}^-$  in case of Ca/Na-1 and  $\text{Cl}^-$  and  $\text{OH}^-$  in case of  $\text{CaCl}_2 \cdot 2\text{H}_2\text{O}$ ).<sup>15</sup>

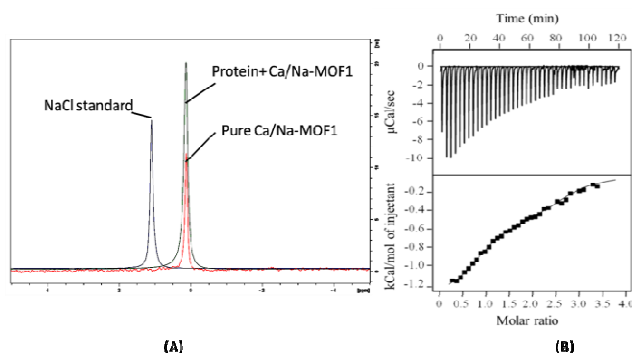


Figure 3. (A) Overlay of  $^{23}\text{Na}$  spectra of pure Ca/Na-1, NaCl standard and M-crystallin Protein+ pure Ca/Na-1 solution (B) ITC thermogram of Ca/Na-1 titration with M-crystallin. Protein concentration was  $60\ \mu\text{M}$  in  $25\ \text{mM}$  Tris-HCl buffer, pH 7.4 and  $100\ \text{mM}$  NaCl.

Stoichiometry of binding was estimated from a suite of NMR titrations carried out using different protein: Ca/Na-1 concentrations (1: 0.5, 1:1, 1:2 and 1:3). Saturation of both the  $\text{Ca}^{2+}$  binding sites was observed with 1:3 protein to Ca/Na-1 ratio. It is speculated that  $\text{Ca}4$  is dislodged from Ca/Na-1 due to higher energy of  $\text{Ca}[\text{H}_2\text{O}]_4^{2+}\cdot 2\text{H}_2\text{O}$  in co-ordination sphere.<sup>16</sup> Thereby,  $2\text{Ca}^{2+}$  are re-released per 3 molecules in order to saturate the binding sites on protein. MALDI-TOF mass spectrum of protein with Ca/Na-1 in 1:2 ratio showed  $[\text{M}+\text{H}]^+$  at  $m/z$  9259.12 and 9390.81, which correspond to apo and holo protein respectively (Figure 4A). It was also observed that bond length and bond angle parameters contributed to the release of  $\text{Ca}^{2+}$  ions. The bond length of Ca(4)-O(26), Ca(4)-O(11), Ca(4)-O(12), Ca(4)-O(7) (2.510-2.560 Å) were found larger as compared to other Ca-O bond lengths (2.359-2.487 Å). It supported that larger bond length of Ca(4)-O bond per unit composition of the complex as depicted in Fig 1A, facilitated its release. Further, the smaller bond angle of O(27)-Ca(4)-O(11) contributes to spontaneous release of Ca.

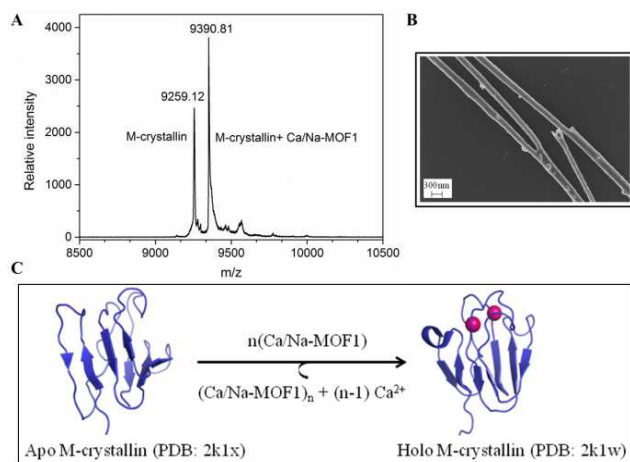


Figure 4. (A) Representative MALDI-TOF mass spectrum of M-crystallin titration with Ca/Na-1 at 1:2 ratio of protein vs Ca/Na-1. (B) FE-SEM image of Ca/Na-1 after  $\text{Ca}^{2+}$  release. (C) Schematic showing  $\text{Ca}^{2+}$  release from Ca/Na-1 and conversion of apo M-crystallin to holo form.

A mass difference of 131.69 supports the chelation of two  $\text{Ca}^{2+}$  ions along with three water molecules. Post binding Ca/Na-1, undergoes polymerization to form branched, porous nanorods with an average length of  $\sim 3\ \mu\text{m}$  and mean diameter of  $\sim 200\ \text{nm}$  as observed in the FE-SEM imaging (Figure 4B). M-

crystallin/Ca/Na-1 complexation is schematically illustrated in Figure 4C. The nanorods thus formed disintegrate within  $\sim 48\ \text{hrs}$  ensuring degradability in physiological conditions.

The results demonstrate the utility of calcium-sodium based coordination polymer which mimics the role of  $\text{Ca}^{2+}$  buffers in living cells, as corollary to  $\text{Na}^+/\text{Ca}^{2+}$  exchange proteins (NCX) that act in reversible fashion to maintain concentration gradients of individual ions across membranes. NCX bind to  $\text{Ca}^{2+}$  with low affinity but can transport as many as 5000 ions per second, making them fast dispensers of the ion during generation of action potential for nerve impulse or signal transduction.<sup>17</sup> Disruption in functioning of these proteins and subsequent low blood  $\text{Ca}^{2+}$  levels lead to adverse effects including neurological impairment, seizures, abnormal heart rhythm and certain cancers.<sup>18</sup> In such cases, developing simple strategies to replenish  $\text{Ca}^{2+}$  levels becomes indispensable for averting the complications.

In summary, we propose that EGTA based coordination polymer forms an apt system to incorporate biologically relevant metal ions for targeted metal ion delivery to proteins. In terms of synthesis, Ca/Na-1 is obtained in aqueous solutions, instead of organic solvents. In this particular case, Ca/Na-1, EGTA serves as a biological mimic of  $\text{Ca}^{2+}$  buffer. In addition to  $\text{Ca}^{2+}$  ion chelation by EGTA, the Ca/Na-1 seems to release felicitous amounts of  $\text{Ca}^{2+}$  ions at designated target sites on protein. Thus, Ca/Na-1 can be readily deployed to sequester  $\text{Ca}^{2+}$  for selective manipulation of cellular  $\text{Ca}^{2+}$  levels and associated physiological functions.

## Notes and references

<sup>a</sup> Department of Chemistry, Banaras Hindu University, Varanasi- 221005, India e-mail:lmishrabhu@yahoo.co.in Ph: +91-542-6702449, Fax: +91-542-2368127

<sup>b</sup> Department of Chemical Sciences, Tata Institute of Fundamental Research, Mumbai- 400005, India.

† Electronic Supplementary Information (ESI) available: Detailed experimental procedures include synthesis, crystallographic data, bond length, bond angle data, MALDI-TOF mass spectrum, NMR spectra, UV-vis and emission spectra of Ca/Na-1, comparison of M-crystallin titration using Ca/Na-1 and  $\text{CaCl}_2$  as titrant, and thermodynamic parameters of M-crystallin- Ca/Na-1 complexation. CCDC no. 981423, crystallographic data in CIF or other electronic format see DOI: 10.1039/b000000x/ RG and LM thank CSIR, New Delhi, India for financial assistance. AS thanks ICMR, India for the SRF. Mr. Rudheer Bapat is acknowledged for the help with FE-SEM imaging.

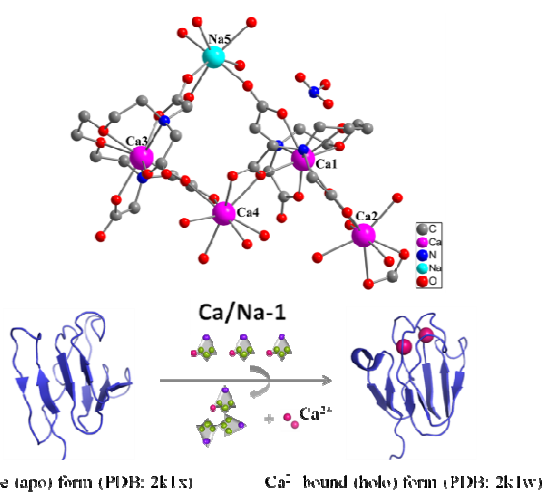
\*These authors contributed equally.

## REFERENCES

- (a) C. Janiak *Dalton Trans.*, 2003, 2781–2804; (b) R. Chakrabarty, P. S. Mukherjee and P. J. Stang, *Chem. Rev.* 2011, **111**, 6810–6918; (c) Z. Ma and B. Moulton *Coord. Chem. Rev.* 2011, **255**, 1623–1641; (d) E. Coronado, C. Martí-Gastaldo, J. R. Galán-Mascarós and M. Cavallini, *J. Am. Chem. Soc.* 2010, **132**, 5456–5468; (e) Y. Yan and J. Huang, *Coord. Chem. Rev.* 2010, **254**, 1072–1080; (f) Janiak, C. *Angew. Chem. Int. Ed.* 1997, **36**, 1431; (g) D. Tanaka, A. Henke, K. Albrecht, M. Moeller, K. Nakagawa, S. Kitagawa and J. Groll, *Nature Chemistry* 2010, **2**, 410–416.
- (a) A. Y. Robin and K. M. Fromm *Coord. Chem. Rev.* 2006, **250**, 2127–21573; (b) X. Zhang, L. Hou, B. Liu, L. Cui, Y. -Y Wang, and B. Wu *Cryst. Growth Des.* 2013, **13**, 3177–3187; (c) G. -Z. Liu, X. -D. Li, X. -L. Lia and L. -Y Wang *Cryst. Eng. Comm.*, 2013, **15**, 2428–2437; (d) S. Neogi, J. A. R. Navarro, and P. K. Bharadwaj *Cryst. Growth Des.* 2008, **8**(5), 1554–1558.
- (a) J. A. R. Navarro, E. Barea, J. M. Salas, N. Masciocchi, S. Galli, A. Sironi, C. O. Aniad and J. B. Parrad *J. Mater. Chem.*, 2007, **17**,

- 1939–1946 (b) J. S. Hu, X. Q. Yao, M. D. Zhang, L. Qin, Y. Z. Li, Z. J. Guo, H. G. Zheng and Z. L. Xue, *Cryst. Growth Des.* 2012, **12**, 3426–3435. (b) J. D. Lin, J. W. Cheng and S. Du, *W. Cryst. Growth Des.* 2008, **8**, 3345–3353. (c) L. J. Murray, M. Dinca, J. Y. S. Chavan, S. Bordiga, C. M. Brown and J. R. Long, *J. Am. Chem. Soc.* 2010, **132**, 7856–7857.
4. (a) C. S. B. Gomes, D. Suresh, P. T. Gomes, L. F. Veiros, M. T. Duarte, T. G. Nunes and M. C. Oliveira *Dalton Trans.*, 2010, **39**, 736–748; (b) F. Novio, J. Simmchen, N. Vázquez-Mera, L. Amorín-Ferré, D. Ruiz-Molina *Coord. Chem. Rev.* 2013, **257**, 2839–2847; (c) X. Yuan, X. Zhang, H. Zhao, L. Liu, and B. Wu *Cryst. Growth Des.* 2013, **13**, 4859–4867; (d) F. Setifi, E. Milin, C. Charles, F. Thetiot, S. Triki and C. J. Gomez-García, *Inorg. Chem.* 2014, **53**, 97–104; (d) E. Alvarez, A. G. Marquez, T. Devic, N. Steunou, C. Serre, C. Bonhomme, C. Gervais, I. Izquierdo-Barba, M. Vallet-Regi, D. Laurencin, F. Maurif and P. Horcajada, *Cryst. Eng. Comm.*, 2013, **15**, 9899–9905.
5. (a) M. Collot, C. Loukou, A. V. Yakovlev, C. D. Wilms, D. Li, A. Evrard, A. Zamaleeva, L. Bourdieu, J. -F. Léger, N. Ropert, J. Eilers, M. Oheim, A. Feltz and J. -M. Mallet, *J. Am. Chem. Soc.* 2012, **134**, 14923–4931; (b) S. R. Miller, E. Alvarez, L. Fradcourt, T. Devic, S. Wuttke, P. S. Wheatley, N. Steunou, C. Bonhomme, C. Gervais, D. Laurencin, R. E. Morris, A. Vimont, M. Daturi, P. Horcajada and C. Serre, *Chem. Commun.* 2013, **49**, 7773–7775.
- 20 25 6. J. Hong and P. N. Pintauro, *Water, Air, Soil Pollut.* 1996, **87**, 73–91.
7. A. C. H. Durham *Cell Calcium* 1983, **4**(1), 33–46.
8. P. Liang, H. -K. Liu, C. -T. Yeh, C. -H. Lin and V. Zima, *Cryst. Growth Des.*, 2011, **11**, 699–708.
9. A. L. Spek, PLATON: *Acta Crystallogr., Sect. D*, 2009, **65**, 148–155.
- 30 10. (a) N. Kumari, R. Prajapati, O. Hayashida and L. Mishra, *Polyhedron* 2010, **29**, 2755–2761. (b) S. Gao, M. -L. Chen and Z. -H. Zhou, *Dalton Trans.*, 2014, **43**, 639–645.
11. S. Schmatloch, M. F. González, U. S. Schubert, *Macromol. Rapid Commun.* 2002, **23**, 957–961.
- 35 12. P. Liang, H. -K. Liu, C. -T. Yeh, C. -H. Lin, V. Zima, *Cryst. Growth Des.*, 2011, **11**(3), 699–709.
13. R. P. Barnwal, M. K. Jobby, K. M. Devi, Y. Sharma and K. V. R. Chary *J. Mol. Biol.* 2009, **386**(3), 675–89.
- 40 14. P. Aravind, S. K. Suman, A. Mishra, Y. Sharma, and R. Sankaranarayanan *Biochemistry* 2009, **48**, 12180–12190.
15. Y. Ogawa and M. Tanokura, *J. Biochem.* 1984, **95**(1), 19–28.
16. A. K. Katz, J. P. Glusker, S. A. Beebe and C. W. Bock. *J. Am. Chem. Soc.* 1996, **118**, 5752–5763.
17. R. Dipolo and L. Beaugé, 2006, **86**(1), 155–203.
- 45 18. I. Bezprozvany, *Trends Mol Med.* 2009, **5**(3), 89–100.

## TOC



50 Ca<sup>2+</sup> free (apo) form (PDB: 2k1s) Ca<sup>2+</sup> bound (holo) form (PDB: 2k1w)